Methods for Verification of Virtual Prototypes of Mining Machines for Strength Criterion

Jarosław Tokarczyk

Abstract—**Methods for verification of virtual prototypes of powered roof support and falling object (FOPS) protective structure for operator for strength criterion were presented in the paper. In the case of powered roof support resistance strain gauge measurements and geometrical measurements were used. Method of building of computational models and their further modifications for the purpose of comparison of results was presented. Potential reasons of differences between results of stand tests and results of virtual tests were showed. Virtual prototype of FOPS protective structure was verified with use of reverse engineering (RE) method.**

Index Terms— **Virtual prototyping, finite element method, reverse engineering, stand test, numerical methods**

I. INTRODUCTION

EACH machine or equipment in the Polish hard coal mining industry before its actual use should be subjected to a series of obligatory stand tests, on the basis of which Notified Body makes assessment of product conformity.

Depending on a type and range of use of a given machine or equipment, there is a different range of required tests. Each machine designed for operation in underground mining industry, e.g. machine that belongs to so-called longwall system, is subjected to strict strength tests at the stage of product certification. Most of the tests belong to non-destructive tests, after which a given machine can not be used. In the case of not meeting the assumed requirements it is necessary to manufacture the next copy of the material prototype. Due to this, at present before final manufacturing of machine or equipment, which is designed for stand tests, virtual prototyping is applied. Virtual tests, which are conducted in this way at the KOMAG Institute of Mining Technology (Poland), minimize a risk of not meeting the assumed requirements during conducting of experimental tests. On the other hand, results of experimental tests are the basis for verification of virtual prototypes. Due to higher and higher possibility of complication of virtual prototype, which results from increasing computational power of present computers and development of the next versions of software of CAE (*Computer Aided Engineering*) class, it is possible to create complex finite element meshes of computational models and

to simulate wide range of physical phenomena [14]. However, it requires continuous verification of virtual prototypes with the results of stand tests. Verification of virtual prototype for strength criterion [15], with use of the following measuring methods: resistance strain gauge measurements, geometrical measurements and RE, was presented in the paper on the basis of powered roof support and FOPS.

II. POWERED ROOF SUPPORT

Powered roof supports have to protect workers against roof fall during underground mining of hard coal by a longwall system, which is especially popular in Poland and in Europe [17]. Powered roof supports are a part of longwall system, including also longwall shearer with flight-bar conveyor.

Main components of powered roof support are as follows, Fig. 1:

    --Base (1).
    --Canopy (2).
    --Gob shield (3).
    --Hydraulic legs (4).
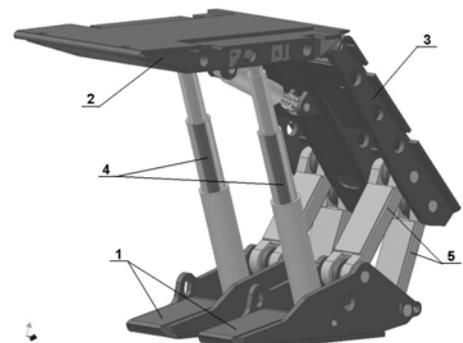   --Lemniscate links (5).

Fig. 1. 3D geometrical model of powered roof support.

Links with gob shield make the lemniscate system, which ensures rectilinear, vertical movement of canopy in a required range of height of support.

A. Virtual prototyping

On the basis of 3D geometrical model a solid computational model of powered roof support was created. Boundary conditions of computational model were in accordance with support scheme A.1.1a − A.2a, according to [10] Table 1.

Due to this, computational model consisted of the following:

    --716081 nodes.
    --396443 TET10 solid elements.

--48 MPC elements (articulated joints).

Type of supporting	Scheme of supporting	
	Canopy	Base
A.1.1a-A.2a		

--4 MPC elements (supports).
--24 beam 1D elements (bolts).
--38 beam 1D elements (virtual strain gauges).

Linear-and-elastic model of material of the following properties was assumed:

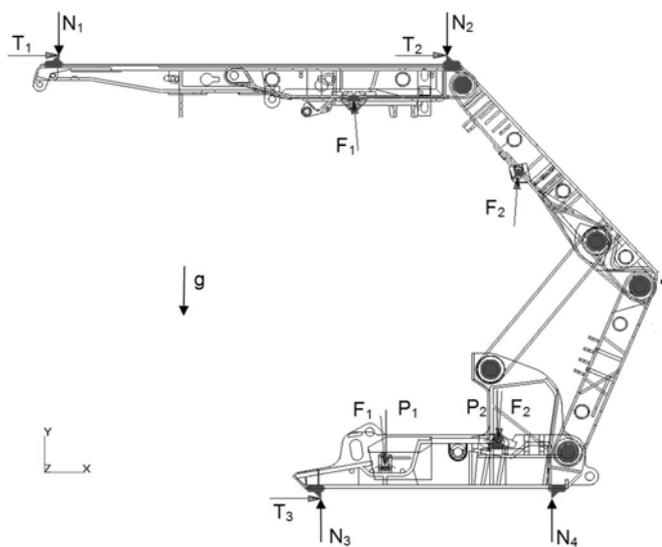--Young's modulus – 205 [GPa].
--Poisson's ratio – 0.3.

Fig. 2. Boundary conditions of computational model of powered roof support.

--Density – 7850 [kg/m3].

According to passive load, forces coming from front hydraulic legs F_1 and back hydraulic legs F_2, Fig. 2.

Values of forces were calculated on the basis of pressure in under-piston areas of hydraulic supports during stand tests. Forces coming from masses of front legs m_1, back legs m_2, canopy m_3 and gob shield m_4 acted on the base. Frictional forces between supporting beam and roof T_1, T_2 and supporting beam and floor T_3 were determined in supports, in which movement along OX axis is possible. Vectors of frictional forces were directed in opposite direction to the movement of a given support. Calculation of frictional forces (base – floor, canopy – roof) required making of initial calculations for each load variant.

Values of active forces, which are in computational model of exemplary support were as follows:

--F_1= 1.72 [MN].
--F_2= 1.22 [MN].
--$T_{1,2,3}$= N1,2,3 * μ.
--P_1=m_1*g + m_3*g.
--P_2=m_2*g + m_4*g.

Where: m_1=615 [kg]; m_2=368 [kg]; m_3=5270 [kg]; m_4=4030 [kg]; m_4=4030 [kg]; μ = 0.1 – steel – steel friction coefficient; N – calculated values of reactions in points of support. These values depend on a variant of support of powered roof support model.

--g – direction of gravity.

Additionally, virtual strain gauges (measuring points of deformations) were created in the computational model. These were beam elements of BEAM2 type of radius equal to 10^{-6} [m]. They had common nodes with TET10 solid elements to obtain identical values of deformations.

Beam elements were placed in accordance with the placement of measuring strain gauges on a real object.

B. Stand tests

According to the European standard requirements [10], within strength criterion, the tests of powered roof supports include a cycle of static and fatigue loads at the test stand prepared specially for that purpose. Such a stand is at the KOMAG Institute of Mining Technology, Fig. 3.

Bearing structure of the stand consists of four frames (1), which at the same time are the guide rails for four traverses (2) and roof (3). The roof is of box structure, where all hydraulic cylinders have jointed bearings. The roof transfers vertical loads acting on tested powered roof support. The load is exerted by 12 hydraulic cylinders (4) of Ø 250 [mm] diameter, which are articulately supported in traverses and in roof. Control of all operations related to the operation of test stand (change of roof height, vertical load of support, horizontal sliding of floor) is realized from control panel.

Conditions of testing are determined by the following:
--Methods of supporting of bases.
--Methods of supporting of canopy.
--Methods of support loading: passive, active.

Stand tests, by suitable methods of loading of powered roof support, i.e. methods of supporting of canopy and bases, recreate real conditions of mining in laboratory conditions in a simplified way. According to standard assumptions, different methods of supporting of powered
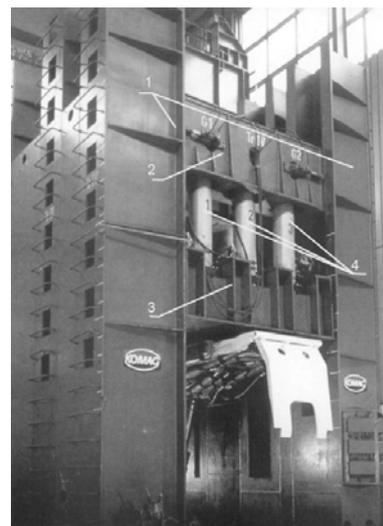

Fig. 3. Stand for testing of powered roof supports located at the KOMAG Institute of Mining Technology.

roof support, which are applied during static tests, can be distinguished. Selection of proper methods of supporting of the system depends on a structure of tested powered roof support. Passive load of support is realized by supplying the hydraulic components, which decide about load bearing

capacity of support, i.e. hydraulic legs, canopy cylinder. Active load of the support system is realized by acting of stand roof on the support with simultaneous control of increase of pressure in hydraulic components of support. Both methods enable gradual increase of support load.

Applied programmes of loading of powered roof support include symmetrical and asymmetrical methods of roof supporting.

During static stand tests of powered roof support the measurements of the following amounts, which characterize load condition of support, are made:

--Values of strains in selected points of support sub-systems.

--Deflections (deformations) of basic support sub-systems (bases, gob shield, canopy).

--Pressure in operational spaces of hydraulic components (legs, canopy cylinder).

C. Comparative analysis of results of calculations and measurements

Observed differences between results of stand tests and FEM calculations are caused mainly by arrangement of measuring and virtual strain gauges close to the places where there is a high gradient of material deformation. Moreover, discretization errors may additionally occur in those places. Such errors appear in finite elements, geometrical form of which is degenerated, i.e. in flattened or shapeless elements. In the case of geometrically complex computational models degenerated elements are in roundings of small radius, bevelling of edges, precise mapping of screws in holes, notches, etc. Discretization error appears by high gradient of resulted values between each node of a single degenerated finite element.

Elimination of discretization errors requires re-making of FEM calculations within global-and-local task, which is solved in this model area where such error occurred. Solving of the task begins with densification of FEM mesh in a given part of tested computational model. Moreover, geometrical model can not have the features, which make creation of consistent finite elements mesh impossible. It is difficult to identify them, especially in expanded geometrical models, such as: installation clearances, edge adhesion of metal sheets and tangential connection of cylindrical surface and flat surface.

1) Global task

Global task includes computational model, which comprises all sub-systems of analyzed machine or equipment. Tensors of axial deformation of measuring and virtual strain gauges were compared. Obtained results are presented in a form of diagram, Fig. 4.

Value of deformation of measuring strain gauge and beam component is presented on a diagram on OY axle. Numbers of measuring strain gauges are on OX axle.

Differences between values of deformations of virtual and real strain gauges result from the following reasons:

--Strain gauges are placed in areas of high gradient of reduced stresses, where even a small change of placement of measuring point is manifested by a big difference in the results (Fig. 5 area A).

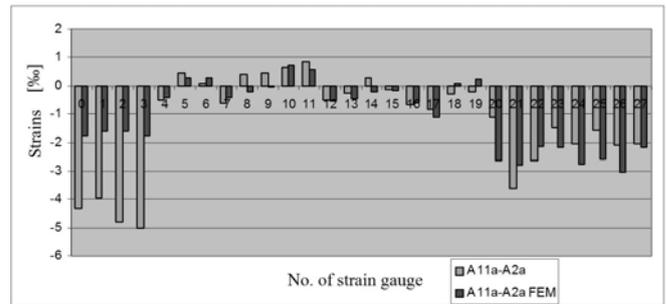--There are differences between placement of real and

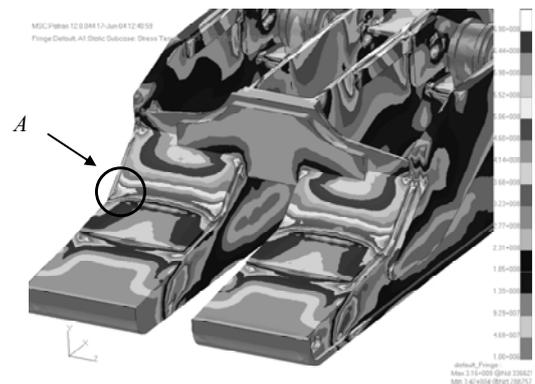Fig. 4. Comparison of values of strains in measuring points for A.1.1a – A.2a support type.

Fig. 5. Map of reduced stresses on a base, isometric view.

virtual strain gauges. These differences result form uncertainty of measurement of placement of strain gauges on a powered roof support.

--Computational model is made strictly according to the documentation, while in a real object there are inaccuracies associated with tolerance of manufacturing and clearances in bolt connections. These factors can disturb symmetrical operation of powered roof support.

--There are differences in homogeneity of real material.

--Non-linear behaviour of material after exceeding of yield point was not included.

--At test stand the roof is supported by 12 cylinders – there is a possibility of temporary non-parallelism of roof and base.

Comparison of deformations (deflections) of the whole systems of powered roof support is the other method for verification of virtual prototype for strength criterion. Values of deflections of base and canopy are measured on their side edge. Deflection is a relative value between vertical displacement of canopy ends or base ends and vertical displacement of the middle part of the edge. During stand tests location of measuring point at the edge of base or canopy is initially estimated and corrected during strength tests. To obtain maximal value of deflection for a given component it is required to determine deflection diagram.

Comparison of differences between maximal deflections of canopy and base obtained from calculations and stand tests is included in Table 2.

Results obtained from FEM calculations were modified to read the value of gob shield deflection. It was necessary because of movement and rotation of gob shield, in the case of each method of supporting of powered roof support, what made direct reading of deflection impossible.

Due to that, application started in the environment of AutoCad software was created for that purpose. There were

the following input data to the programme:

--Deformed, surface FEM mesh of gob shield upper surface.

--Coordinates of reference node.

TABLE II
COMPARISON OF VALUES OF DEFLECTIONS OF BASE AND CANOPY OF EXEMPLARY POWERED ROOF SUPPORT

Type of supporting	Component	Deflection value [mm]		Difference [%]
		Stand tests	FEM calculations	
A.1.1a –	Base	5.4	5.11	5.37
A.2a	Canopy	17.6	20.81	18.18

The reference node was created in the middle of diagonal of gob shield upper surface and its location was in accordance with measuring point at test stand, Fig. 6.
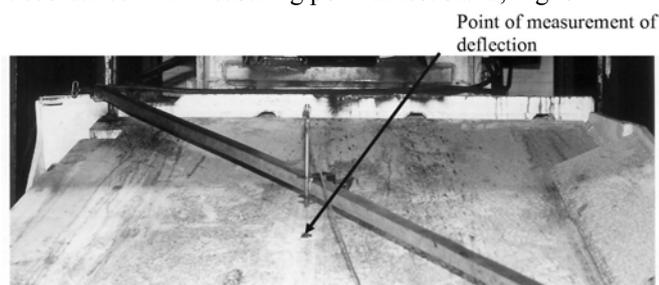

Fig. 6. Point of measurement of deflection at test stand.

Deformed FEM mesh and coordinates of node were exported in a file of Patran Neutral File format. The results are shown in the Table 3.

TABLE III
COMPARISON OF VALUES OF GOB SHIELD DEFLECTIONS FOR EXEMPLARY POWERED ROOF SUPPORT

Type of supporting	Value of gob shield deflection [mm]		Difference [%]
	Stand tests	FEM calculations	
A.1.1a – A.2a	2.7	2.13	21.11

Difference between deflection value that was calculated and deflection value obtained on the basis of stand tests was observed. Clearances present in bolt connections and tolerance of manufacturing of each part were not included in computational model. Average value of deflection obtained from stand tests is equal to 2.05 [mm], while value of clearance in bolt connection is equal to $1 - 2$ [mm] between diameter of hole and diameter of shaft, due to what they have an impact on obtained results [9].

Insensitivity to discretization errors is an advantage of the method of verification by comparison of deflections of each sub-system. Additionally, value of deflection of a given system is a determinant of its global exerting and this result is not disturbed by local differences in values of stresses, what happens in the case of strain gauge measurements.

2) Local task

A part of computational model, which requires local densification of the mesh and more accurate representation of design form, is extracted from the whole, and treated as a separate task, including the boundary constrains that connect it with the surrounding. These constrains are represented by displacements. In the latest versions of computational software local task is a part of global task and it is solved simultaneously.

For the task needs elastic-and-plastic model of material with linear strengthening of the following properties corresponding to material, which was used in powered roof support, was defined:

--Young's modulus – 205 [GPa].

--Poisson's ratio – 0.3.

--Density – 7850 [kg/m^3].

--Yield point – 690 [MPa].

--Strength – 930 [MPa].

--Elongation – 10%.

Due to the time of calculations, material of these properties was assigned only to the small part of local model, in which exceeding of yield point should have been expected. Linear-and-elastic properties were assigned to the rest part of the model.

Selected parts of the model were covered with the mesh of TRIA6 surface elements of the thickness equal to 10^{-6} [m]. This mesh is stretched in a local coordinate system, in which one of the axles is in accordance with a direction of virtual strain gauge. Elements of the mesh had joint nodes with TET10 elements of solid model, what caused identical deformations.

Ranges of fields of deformations close to strain gauges were obtained in a result of solving of global-and-local tasks with use of surface mesh. Comparison of values of deformations of measuring strain gauges with the ranges of fields of deformations obtained for surface elements is given in Table 4. "-" sign means compression. The ranges in perpendicular direction to longitudinal axis of assessed strain gauge were compared.

TABLE IV
RANGES OF FIELDS OF DEFORMATIONS AROUND EACH ELONGATION MEASURING POINT

No. of measuring strain gauge	Elongation of measuring strain gauge (stand tests) [‰]	Range of field of deformation around measuring strain gauge [‰]
4	-0.49	-0.1 ÷ 1.75
5	0.46	-5.9 ÷ 7.45
8	0.41	-1.96 ÷ 0.488
14	0.26	-0.426 ÷ 0.2
16	-0.68	-1.14 ÷ -0.36
17	-0.85	-2.95 ÷ -0.494
18	-0.31	-1.66 ÷ 2.6
19	-0.22	-2.00 ÷ 1.52
20	-1.11	-4.77 ÷ 0.733

Obtained results confirm sensitivity of result of deformation to change of strain gauge location. Due to the above, use of several independent methods of verification is required to verify virtual prototype with the results of stand tests and to obtain objective comparison. In some cases it is indispensable to use RE method.

III. FALLING OBJECT PROTECTIVE STRUCTURE (FOPS)

FOPS and ROPS (*Roll-Over Protective Structures*) types, which protect operators of self-propelled vehicles are used

in the mining industry. FOPS protects the operator against falling rock slides, while ROPS protects against crushing during vehicle overturn. These structures are subjected to destructive tests, according to standards, which are in force [11, 13]. ROPS are also used in general automotive industry [1] and in special vehicles. The results of virtual prototyping of protective structure for the operator of side-discharge loader are verification subject. Verification for strength criterion was conducted, i.e. protective structure was loaded by falling weight.

A. Virtual prototyping

FOPS virtual prototyping for safety criterion was conducted by FEM method in MSC.Dytran software environment [3]. Non-linear, time-dependent calculations were carried out. Nonlinearities resulted from taking into account contact phenomena and elastic-and-plastic phenomena of material model. Computational model for the weight and FOPS protective structure was developed. A model of weight of 520 [kg] consisted of 6074 TETRA 4 solid elements. Initial distance between the weight and upper sheathing of FOPS was equal to 1 [mm]. A model of weight had initial speed equal to 6.67 [m/s], what corresponds to free fall from the height of 2.3 [m] from upper surface of upper sheathing of FOPS, to obtain impact energy of 11600 [J].

The following simplifications were assumed, basing on experience from previously realized work [2, 5, 7, 8]:

--Computational model consisted of QUAD 4 and TRIA 3 shell elements.

--Grooved joints of sheets were replaced by finite elements of thickness equal to total thickness of sheets in a given joint.

The following material properties were defined:

--Model of material: elastic-and-plastic,
--Young's modulus $E = 2.068*10^{11}$ [Pa].
--Poisson's ratio $\eta = 0.29$.
--Yield point $Re_{min} = 330$ [MPa].
--Tensile strength $Rm = 490 \div 630$ [MPa].

The same supporting method as for the object at test stand: rigid anchoring at the lower edges of vertical supports, was assumed for the computational model.

Calculation process was stopped, when the model of weight reached the speed equal to 0 [m/s], i.e. when the verified construction took over the whole impact energy (maximal values of displacements and stresses were reached). Values of displacements and stresses present in FOPS structure were obtained in a result of calculations. Displacements of node on the surface of lower sheathing of FOPS, over operator's head, were assumed as criterial ones.

Maximal deflection (elastic and plastic strain) of lower sheathing was equal to 10 [mm] and it did not exceed the value of 50 [mm] determined in a Standard as permissible value. Maximal deflection was equal to 41 [mm] in the place of weight drop after 0.01152 [s] from the time of drop.

B. Stand tests

Conducted laboratory tests aimed at checking of protective structure for operator of loader against local puncture caused by impact load and indirectly by a method for verification of ability of transferring of impact load [6]. The tests were conducted according to the Standard requirements that are in force [11]. Under lower sheathing of structure, at the place of operator's seat a DLV (*Deflection - Limiting Volume*) model of space of dimensions determined in the Standard [12], which can not be affected by deformable parts of the structure and by the weight itself, is placed. View of test stand and geometrical model of FOPS structure and DLV model are presented in
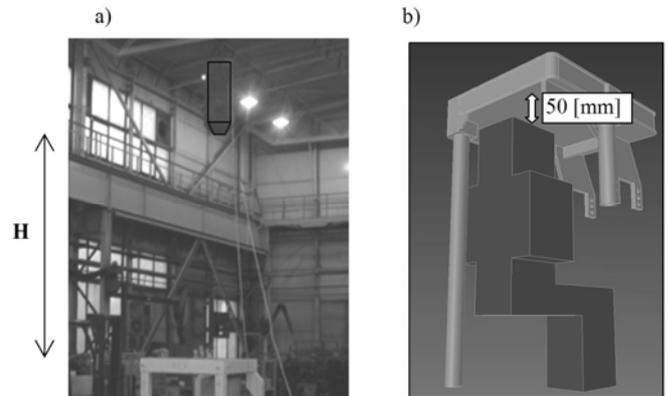

Fig. 7. View of test stand (a) and geometrical model of DLV structure (b).

Fig. 7.

The weight was hanged on a crane hook. The outline of the weight was marked with a line to improve clarity of the picture. According to the Standard the energy of weight impact should be equal to 11 600 [J]. It requires lowering of the weight of 520 [kg] from the height H = 2.3 [m]. Microexplosive, which rapidly breaks hoisting rope of the weight, is used for that purpose.

C. Comparison of results

A reconstruction of upper sheathing after stand tests was conducted by RE method [16] to verify virtual prototype of
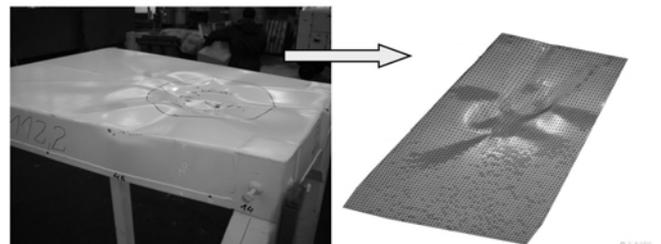

Fig. 8. Surface model of damaged protective structure – RE method.

FOPS structure, Fig. 8.

This method is used for reconstruction of real objects in computer environment. Coordinate measuring machines, optical methods or laser scanning are used in RE method.

At the same time initial positions of nodes of finite elements mesh was modified in FEM postprocessor on the basis of magnitudes and directions of displacement vectors, obtained from deformed upper sheathing of the same FOPS structure, Fig. 9. It is one of functions of present postprocessors [4].
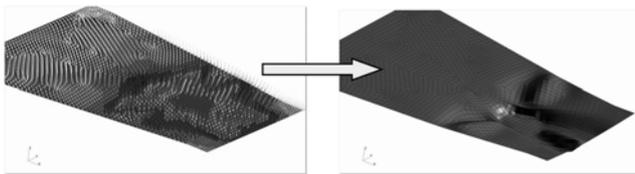
Fig. 9. Modification of positions of nodes of computational model mesh – result of simulation.

Shell models obtained form different sources were presented together to compare displacements of 25 points located in the same places, Fig. 10.
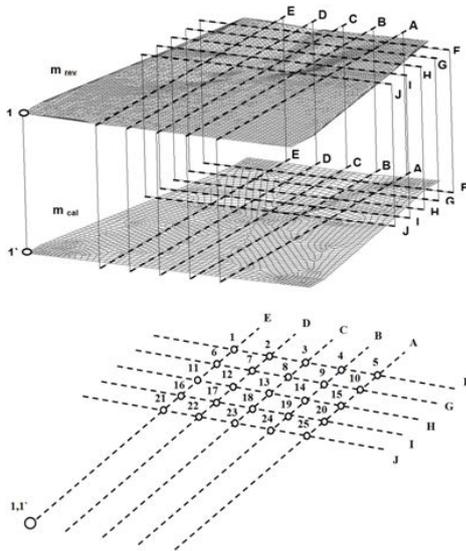

Fig. 10. Presentation of values of displacements of crossing points 1-25.

Significant differences in displacement values result from repeated bounces of the weight during stand tests.

These phenomena were not included in computational model, due to the time of calculations. Use of RE method enabled verification of calculations results by comparison of two geometrical models obtained from two different sources. This method is especially useful in the case of damaged objects of irregular shape, where use of traditional measuring methods is difficult.

IV. SUMMARY

Verification of the virtual prototype enables to identify the reasons of differences between results obtained during simulation and tests on a test stand. Verified virtual prototype enables to assess future machine or equipment in conditions, which can not be obtained at test stand or which are difficult to be obtained. High cost of stand tests, especially in the case of destructive tests in a unit production increases the final price of product that is sold. Additionally, it is required to repeat the test in the case of its negative result, what needs manufacturing of the next material prototype.

Work as regards virtual prototyping for strength criterion

has been conducted at the KOMAG Institute of Mining Technology for more than 10 years. In this time a lot of research work on the basis of which the most significant reasons of differences between results obtained from simulation and stand tests was carried out.

The following factors have the biggest impact on differences between results obtained from virtual prototyping and stand tests:

--Differences between dimensions of geometrical model and real object.

--Boundary conditions.

--Material properties.

--Simplifications of computational model.

--Discretization errors.

Constant and methodical process of verification of virtual prototype enables to develop a method for creation of computational model, on the basis of which results of acceptable error are obtained for identified loading conditions. In this way in the next step it will be possible to use computational methods for certification of such products, which at present require obtaining of positive results of strength tests at test stand. Taking into account increasing possibilities of CAE software, newly designed machines and equipment will be multi-criterially assessed and optimized.

REFERENCES

[1] Z. Barszcz "Ocena bezpieczeństwa dużych pojazdów do przewozu osób w zakresie wytrzymałości ich konstrukcji nośnej". Konferencja: *Spotkanie użytkowników oprogramowania MSC*. Mszczonów 2006. (in Polish)

[2] S. Bojara, Ł. Całus, J. Tokarczyk "Modelowanie wybranych zjawisk dynamicznych na przykładzie struktur ochronnych maszyn samojezdnych". Materiały na konferencję KOMTECH: *Nowoczesne, niezawodne i bezpieczne systemy mechaniczne w świetle wymagań Unii Europejskiej*. Szczyrk 2003. (in Polish)

[3] *MSC.Dytran 2008r1: Theory manual*. MSC.Software Corporation.

[4] Patran® 2010: *Finite element modeling*. MSC.Software Corporation.

[5] Praca badawcza E/BDC – 8403/OR7: *Obliczenia wytrzymałościowe MES kabiny operatora zgodnie z normą PN-EN 13627:2002*. CMG KOMAG, Gliwice 2006. Unpublished. (in Polish)

[6] Praca badawcza niepublikowana SP/BDM – 9877: *Badania weryfikacyjne rzeczywistej konstrukcji chroniącej operatora*. CMG KOMAG, Gliwice 2005. In Polish. Unpublished.

[7] Praca badawcza U/BDC-8643/OR: *Obliczenia wytrzymałościowe konstrukcji chroniącej operatora przed spadającymi przedmiotami*. CMG KOMAG, Gliwice 2003. Unpublished. (in Polish)

[8] Praca badawcza U/BDM – 8752/OR: *Badanie daszka ochronnego*. CMG KOMAG, Gliwice 2004. Unpublished. (in Polish)

[9] G. Ober: Wpływ luzów w prototypowych sekcjach obudów zmechanizowanych na tor końca stropnicy. *Maszyny Górnicze* nr 85/2001, pp. 50-54. (in Polish)

[10] PN-EN 1804-1+A1:2010: *Maszyny dla górnictwa podziemnego. Wymagania bezpieczeństwa dla obudowy zmechanizowanej. Część 1: Sekcje obudowy i wymagania ogólne*. Polish Standard. (in Polish)

[11] PN-EN 13627:2002 *Konstrukcje chroniące operatora przed spadającymi przedmiotami, dotyczy maszyn do robót budowlanych ziemnych*. Polish Standard. (in Polish)

[12] PN-EN ISO 3164:2009 – *Maszyny do robót ziemnych. Laboratoryjna ocena konstrukcji chroniących operatora. Wymagania dotyczące przestrzeni chronionej*. Polish Standard. (in Polish)

[13] PN-92/G-59001 – *Samojezdne maszyny górnicze. Konstrukcje chroniące operatora przed obwałami skał. Wymagania i badania*. Polish Standard. (in Polish)

[14] R. Quey, P.R. Dawson, F. Barbe "Large-scale 3D random polycrystals for the finite element method:Generation, meshing and remeshing". *Computer Methods in Applied Mechanics and Engineering*. Volume 200 (2011) pp. 1729–1745.

[15] T. Winkler, J. Tokarczyk "Multi-criteria assessment of virtual prototypes of mining machines". Proceedings: WCECS 2010, World

Congress on Engineering and Computer Science, Volume II, San Francisco, USA, 20-22 October, 2010 pp. 1149-1153.

[16] T. Winkler, J. Tokarczyk, S. Bojara "Use of reverse engineering method in verification of virtual prototypes". *Computer Assisted Mechanics and Engineering Sciences*. Volume 1 (2008) pp. 53-65.

[17] Scientific and business news and events from the Polish and the world of mining www.teberia.pl.